

Benzenedicarbonyl and benzenetricarbonyl linker pyrazolyl complexes of palladium(II): synthesis, X-ray structures and evaluation as ethylene polymerisation catalysts †

Iliia A. Guzei,^{*a} Kelin Li,^b Galina A. Bikzhanova,^a James Darkwa^{*b} and Selwyn F. Mapolie^b

^a Department of Chemistry, University of Wisconsin-Madison, 1101 University Avenue, Madison, WI 53706, USA

^b Department of Chemistry, University of the Western Cape, Private Bag X17, Bellville 7535, South Africa

Received 28th August 2002, Accepted 12th December 2002

First published as an Advance Article on the web 20th January 2003

A series of novel compounds with pyrazolyl rings (pz) linked by benzenedicarbonyl (**L1–L4**) and benzenetricarbonyl (**L5, L6**) have been prepared and structurally characterized. The mutual orientation of their rings was studied by molecular mechanics. These polydentate species react with PdCl₂(NCMe)₂ to yield dinuclear complexes in which the Pd centers coordinate to one or two pz units, a terminal chloride and two bridging chloride ligands. In complex [(3,5-^tBu₂pzcO)₃-1,3,5-C₆H₄]₂Pd₂Cl₂(μ-Cl)₂, the pyrazolyl ligand **L5** acts as a bidentate donor despite the presence of the third pz group. These Pd complexes, when activated with methylaluminoxane (MAO), exhibit activity in ethylene polymerization.

Introduction

Nitrogen-bound metal complexes containing imidazole and imidazole-like ligands, such as pyrazoles are of interest in protein model studies and drug design.¹ In particular, pyrazole (pyrazole = pzH) derivatives have been used to mimic isomeric imidazole coordination in model studies of metalloenzymes.² Drug related work includes bridging pyrazolato platinum complexes as anti-cancer agents.³ The widest application of pyrazoles is observed in geminal poly(1-pyrazolyl) compounds that form versatile ligands.⁴ Geminal poly(1-pyrazolyl) compounds are uninegative ligands with bonding modes ranging from bidentate to tetradentate.⁴ Poly(1-pyrazolyl) ligands are known to stabilize metals in both high and low oxidation states.⁵ Pyrazolyl compounds are dominated by BR and BR₂ linkers as in RB(3,5-R'₂pz)₃⁻ and R₂B(3,5-R'₂pz)₂⁻ (R = H, alkyl, aryl; pz = C₃H₃N₂), with a few that do not have borate linkers. The preparative chemistry of poly(1-pyrazolyl) ligands includes modification of the substituents at the carbon atoms of the pz rings as well as the linkers that hold the pyrazolyl moieties together. The choice of substituents affects the nucleophilicity of the nitrogen atoms and hence the strength of bonding to the ligated metal. Thus, the overall electrophilic nature of the metal complex can be fine tuned by the choice of pz substituents, linkers, or both.

While a variety of substituted pyrazolyl rings in poly(1-pyrazolyl) compounds has been extensively studied,⁴ the modification of linking units has received little attention. In 1980 Mani and Scapacci reported the first example of a non-boron linker poly(1-pyrazolyl) compound by preparing tris(3,5-dimethylpyrazolyl-1-methyl)amine.⁶ This was soon followed by the work of Driessen *et al.* on *N,N'*-(bis(3,5-dimethylpyrazolyl-1-methyl)amino)ethane,^{7a} which demonstrated that the aminoethane linker allowed the ligand to discriminate between metal ions in complex formation due to the modified nucleophilicity of the pz rings. This shows that sterically compact non-borate pyrazolyl ligands discriminate between different metal ions better than their borate congeners.⁷ In a related work, Sorrel *et al.*⁸ reported the use of 2,6-bis[bis(1-pyrazolyl)ethylamino]-*p*-cresol derivatives as ligands for copper. Another class

of poly(1-pyrazolyl) linker compounds is comprised of pyridine, 2,6-bis(1-pyridin-2-ylpyrazol-3-yl)pyridine or benzene,⁹ 1,3-bis(pyrazol-1-ylmethyl)benzene,¹⁰ and tri-substituted benzene.¹¹ Cyclophosphazenes can also be utilized in this role for poly(1-pyrazolyl) compounds as demonstrated by Chandrasekar *et al.*¹² and others.¹³ However, none of the latter affects the donor ability of the nitrogen atoms in the pyrazolyl units considerably.

An interesting property of pz ligand metal complexes is their catalytic activity in oligomerisation and polymerisation of olefins¹⁴ in addition to the ability to activate C–H bonds.¹⁵ For example, in oligomerisation and polymerisation catalysis of olefins, the electrophilicity of [R₂C(pz)₂PdMe]⁺^{14b} (R = Me, Ph) is considered crucial since the first step in the oligomerisation or polymerisation reaction involves the formation of a palladium-olefin complex. In order to increase the catalytic activity of the pz complexes the presence of a strong electrophilic metal is essential.

Recently, we have set out to explore the influence of electron-withdrawing carbonyl groups located between substituted pz ligands and benzene linkers on nucleophilicity of the pyrazolyl nitrogen atoms and their bonding with the central metal in a number of palladium complexes. Here we report the syntheses and structures of the new type of ligands with several pz moieties as well as syntheses, structures, and catalytic activity of Pd complexes bearing these ligands.

Preliminary investigations of these palladium pyrazolyl complexes as ethylene polymerisation catalysts, show the pyrazolyl palladium compounds are able to catalyse this reaction though the catalysts decompose over time.

Experimental

All reactions were performed under a dry, deoxygenated nitrogen atmosphere using standard Schlenk techniques. Et₃N was dried over KOH. Toluene and hexane were dried with sodium/benzophenone and dichloromethane with P₂O₅. 3,5-ditert-butylpyrazole¹⁶ was prepared according to a literature procedure. 3,5-Dimethylpyrazole, 1,2-benzenedicarbonyl dichloride, 1,3-benzenedicarbonyl dichloride and 1,3,5-benzenetricarbonyl trichloride were obtained from Aldrich and used as received. Ethylene (99.9%) was purchased from AFROX (South Africa) and used as received. Methylaluminoxane

† Electronic supplementary information (ESI) available: molecular structures and bond lengths and angles for **L2**, **L3**, **L6** and **2**. See <http://www.rsc.org/suppdata/dt/b2/b208376k/>

(10% wt.) in toluene was purchased from Aldrich and transferred in a glove box. The NMR spectra were recorded on a Gemini 2000 instrument (^1H at 200 MHz, ^{13}C at 50.3 MHz) at room temperature. The chemical shifts are reported in δ (ppm) and referenced to residual proton and ^{13}C signals of deuterated chloroform as internal standard. ^{13}C NMR spectra of polyethylene were recorded in 1,2,4-trichlorobenzene at 115 °C. The number- and weight-average molecular weights (M_n and M_w) and polydispersity (M_w/M_n) of polymers were determined by high temperature gel permeation chromatography (trichlorobenzene, 145 °C, rate = 1.000 mL min $^{-1}$) on a Waters 2000 instrument. These measurements were performed at the Group Technologies Research and Development laboratory of SASOL Polymers. Thermal analyses were performed on a Universal V2.3H TA instrument. Elemental analysis was performed on a Carlo Erba NA analyzer in the Department of Chemistry, University of the Western Cape.

1,3-Bis(3,5-di-*tert*-butylpyrazolyl-1-carbonyl)benzene (L1)

1,3-Benzenedicarbonyl dichloride (0.60 g, 2.07 mmol) was added to a solution of 3,5-di-*tert*-butylpyrazole (1.00 g, 5.56 mmol) in dry toluene (40 mL), followed by the addition of Et_3N (2 mL). A white precipitate formed immediately and the mixture was stirred at 80 °C overnight. Upon cooling and filtration, the filtrate was evaporated to yield an oil, which was chromatographed (silica gel) using CH_2Cl_2 -hexane (4:1) as eluent. The eluate was evaporated to produce a white solid. Yield = 1.00 g, 73%. Anal. Calc. for $\text{C}_{30}\text{H}_{42}\text{N}_4\text{O}_2$: C, 73.43; H, 8.63; N, 11.42. Found: C, 73.75; H, 9.19; N, 11.36%. ^1H NMR (CDCl_3): δ 8.52 (t, 1H, Ph, $^3J_{\text{HH}} = 1.8$ Hz); 8.15 (dd, 2H, Ph, $^2J_{\text{HH}} = 12.2$ Hz, $^3J_{\text{HH}} = 1.8$ Hz); 7.48–7.55 (t, 1H, Ph, $^2J_{\text{HH}} = 12.2$ Hz); 6.17 (s, 2H, 4-pyrazole); 1.46 (s, 18H, 5-*t*Bu); 1.21 (s, 18H, 3-*t*Bu). $^{13}\text{C}\{^1\text{H}\}$ NMR (CDCl_3): δ 168.1; 162.8; 157.7; 135.8; 135.1; 134.1; 127.0; 105.6; 33.1; 32.2; 29.8; 29.7.

Compounds **L2** and **L3** were prepared in a similar fashion.

1,3-Bis(3,5-dimethylpyrazolyl-1-carbonyl)benzene (L2)

This compound was prepared from the reaction of 1,3-benzenedicarbonyl dichloride (2.16 g, 10.40 mmol) and 3,5-dimethylpyrazole (2.00 g, 20.81 mmol). Yield = 2.15 g, 64%. Anal. Calc. for $\text{C}_{18}\text{H}_{18}\text{N}_4\text{O}_2$: C, 67.07; H, 5.63; N, 17.38. Found: C, 67.47; H, 5.57; N, 17.10%. ^1H NMR (CDCl_3): δ 8.57–8.59 (t, 1H, Ph, $^3J_{\text{HH}} = 1.8$ Hz); 8.18 (dd, 2H, Ph, $^2J_{\text{HH}} = 7.8$ Hz, $^3J_{\text{HH}} = 1.8$ Hz); 7.56 (t, 1H, Ph, $^2J_{\text{HH}} = 7.8$ Hz); 6.06 (s, 2H, 4-pyrazole); 2.63 (s, 6H, 5- CH_3); 2.23 (s, 6H, 3- CH_3). $^{13}\text{C}\{^1\text{H}\}$ NMR (CDCl_3): δ 167.3; 152.2; 145.0; 134.8; 134.1; 133.2; 127.2; 111.1; 14.2; 13.7.

1,3-Bis(3-methylpyrazolyl-1-carbonyl)benzene (L3)

This compound was prepared from the reaction of 1,3-benzenedicarbonyl dichloride (2.16 g, 10.40 mmol) and 3-methylpyrazole (1.73 mL, 20.81 mmol). Yield = 2.02 g, 66%. Anal. Calc. for $\text{C}_{16}\text{H}_{14}\text{N}_4\text{O}_2$: C, 65.30; H, 4.79; N, 19.04. Found: C, 66.88; H, 4.59; N, 19.22%. ^1H NMR (CDCl_3): δ 8.88 (t, 1H, Ph, $^3J_{\text{HH}} = 1.9$ Hz); 8.36 (dd, 2H, Ph, $^2J_{\text{HH}} = 8.0$ Hz, $^3J_{\text{HH}} = 1.8$ Hz); 8.33 (d, 2H, 5-pyrazole, $^2J_{\text{HH}} = 2.6$ Hz); 7.64 (t, 1H, Ph, $^2J_{\text{HH}} = 8.0$ Hz); 6.35 (d, 2H, 4-pyrazole, $^2J_{\text{HH}} = 2.6$ Hz); 2.35 (s, 6H, 3- CH_3). $^{13}\text{C}\{^1\text{H}\}$ NMR (CDCl_3): δ 165.0; 154.7; 135.4; 134.6; 131.9; 131.6; 127.8; 110.51; 14.0.

1,2-Bis(3,5-di-*tert*-butylpyrazolyl-1-carbonyl)benzene (L4)

The procedure is similar to that for compound **L1** but using 3,5-di-*tert*-butylpyrazole (2.00 g, 11.09 mmol) and 1,2-benzenedicarbonyl dichloride (0.80 mL, 5.55 mmol). Yield = 1.27 g, 42%. Anal. Calc. for $\text{C}_{30}\text{H}_{42}\text{N}_4\text{O}_2$: C, 73.43; H, 8.63; N, 11.42. Found: C, 73.30; H, 9.76; N, 11.38%. ^1H NMR (CDCl_3): δ 7.80 (dd, 2H, Ph, $^2J_{\text{HH}} = 5.4$ Hz, $^3J_{\text{HH}} = 3.2$ Hz); 7.50 (dd, 2H, Ph, $^2J_{\text{HH}} = 5.9$ Hz, $^3J_{\text{HH}} = 3.3$ Hz); 6.06 (s, 2H, 4-pyrazole); 1.36 (s, 18H,

5-*t*Bu); 1.07 (s, 18H, 3-*t*Bu). $^{13}\text{C}\{^1\text{H}\}$ NMR (CDCl_3): δ 167.9; 162.9; 157.7; 137.5; 130.0; 129.1; 106.1; 33.2; 32.2; 29.6; 29.1.

1,3,5-Tris(3,5-di-*tert*-butylpyrazolyl-1-carbonyl)benzene (L5)

To a solution of 1,3,5-benzenetricarbonyl trichloride (0.50 g, 1.88 mmol) in toluene (60 mL) was added a solution of 3,5-di-*tert*-butylpyrazole (1.02 g, 3.76 mmol) in toluene (20 mL) and Et_3N (2 mL). The mixture was heated at 60 °C for 18 h, filtered solvent removed in *vacuo* give a solid residue which was chromatographed on a silica gel column using CH_2Cl_2 as eluent. Evaporation of the eluate gave analytically pure **L5**. Yield = 0.60 g, 46%. Anal. Calc. for $\text{C}_{42}\text{H}_{60}\text{N}_6\text{O}_3$: C, 72.38; H, 8.68; N, 12.06. Found: C, 71.95; H, 9.32; N, 11.41%. ^1H NMR (CDCl_3): δ 8.80 (s, 3H, Ph); 6.17 (s, 2H, pyrazole); 1.46 (s, 18H, 5-*t*Bu); 1.18 (s, 18H, 3-*t*Bu). $^{13}\text{C}\{^1\text{H}\}$ NMR (CDCl_3): δ 166.2; 152.3; 144.6; 137.0; 132.7; 111.0; 33.2; 32.1; 29.5; 29.3.

Compound **L6** was synthesized in a similar fashion.

1,3,5-Tris(3,5-dimethylpyrazolyl-1-carbonyl)benzene (L6)

This compound was prepared from the reaction of 1,3,5-benzenetricarbonyl trichloride (1.00 g, 3.77 mmol) and 3,5-dimethylpyrazole (1.09 g, 11.30 mmol). Yield = 0.77 g, 46%. Anal. Calc. for $\text{C}_{24}\text{H}_{24}\text{N}_6\text{O}_3$: C, 64.85; H, 5.44; N, 18.91. Found: C, 64.82; H, 5.33; N, 18.43%. ^1H NMR (CDCl_3): δ 8.77 (s, 3H, Ph); 6.55 (s, 2H, pyrazole); 2.64 (s, 6H, 5- CH_3); 2.24 (s, 6H, 3- CH_3). $^{13}\text{C}\{^1\text{H}\}$ NMR (CDCl_3): δ 166.7; 152.6; 145.1; 137.4; 133.1; 111.5; 14.3; 13.9.

Di- μ -chloro-dichloro[1,3-bis(3,5-di-*tert*-butylpyrazolyl-1-carbonyl)benzene]dipalladium(II) (1)

Ligand **L1** (0.42 g, 0.77 mmol) was added to a solution of $[\text{PdCl}_2(\text{NCMe})_2]$ (0.40 g, 1.54 mmol) in CH_2Cl_2 (40 mL). A red, homogeneous solution formed immediately. After stirring for a further 8 h at room temperature, the solvent was evaporated to give a red residue. Recrystallization from CH_2Cl_2 -diethyl ether at -15 °C yielded analytically pure product (0.62 g, 95%) as red crystals suitable for X-ray analysis. Anal. Calc. for $\text{C}_{30}\text{H}_{42}\text{Cl}_4\text{N}_4\text{O}_2\text{Pd}_2$: C, 42.63; H, 5.01; N, 6.63. Found: C, 42.69; H, 4.79; N, 6.60%. ^1H NMR (CDCl_3): δ 9.05 (dd, 2H, Ph, $^2J_{\text{HH}} = 7.8$ Hz, $^3J_{\text{HH}} = 1.8$ Hz); 8.42 (t, 1H, Ph, $^3J_{\text{HH}} = 1.8$ Hz); 8.28 (t, 1H, Ph, $^2J_{\text{HH}} = 7.8$ Hz); 6.36 (s, 2H, 4-pyrazole); 1.83 (s, 18H, 5-*t*Bu); 1.47 (s, 18H, 3-*t*Bu). ^{13}C NMR (CDCl_3): δ 168.8, 168.7, 163.7, 140.5, 136.8, 133.8, 131.7, 109.7, 33.6, 33.4, 31.4, 30.3.

Di- μ -chloro-dichloro[1,3-bis(3,5-dimethylpyrazolyl-1-carbonyl)benzene]dipalladium(II)-dichloromethane (2)

Complex **2** was prepared following the procedure for **1** above but using **L2** (0.25 g, 0.77 mmol) and $[\text{PdCl}_2(\text{NCMe})_2]$ (0.40 g, 1.54 mmol). Recrystallization from CH_2Cl_2 -diethyl ether at -15 °C yielded red crystals suitable for X-ray analysis. Yield = 0.53 g, 96%. Anal. Calc. for $\text{C}_{19}\text{H}_{20}\text{Cl}_6\text{N}_4\text{O}_2\text{Pd}_2$: C, 29.95; H, 2.65; N, 7.35. Found: C, 29.31; H, 2.17; N, 7.36%. ^1H NMR (CDCl_3): δ 8.78 (dd, 2H, Ph, $^2J_{\text{HH}} = 7.9$ Hz, $^3J_{\text{HH}} = 1.7$ Hz); 8.31 (t, 1H, Ph, $^2J_{\text{HH}} = 7.9$ Hz); 7.94 (t, 1H, Ph, $^3J_{\text{HH}} = 1.7$ Hz); 6.27 (s, 2H, 4-pyrazole); 2.76 (s, 6H, 5- CH_3); 2.64 (s, 6H, 3- CH_3). $^{13}\text{C}\{^1\text{H}\}$ NMR (CDCl_3): δ 166.0, 157.5, 150.3, 138.3, 135.2, 133.4, 131.3, 112.7, 16.1, 14.1.

Di- μ -chloro-dichlorobis[1,3-bis(3,5-di-*tert*-butylpyrazolyl-1-carbonyl)benzene]dipalladium(II) (3)

Ligand **L2** (0.50 g, 1.54 mmol) was added to a solution of $[\text{PdCl}_2(\text{NCMe})_2]$ (0.40 g, 1.54 mmol) in CH_2Cl_2 (40 mL). A red precipitate formed immediately. After stirring overnight, the precipitate was filtered off and washed with CH_2Cl_2 to give pure product. Yield = 0.40 g, 52%. Anal. Calc. for $\text{C}_{37}\text{H}_{38}\text{Cl}_6\text{N}_8\text{O}_4$ -

Pd₂: C, 40.98; H, 3.53; N, 10.33. Found: C, 41.05; H, 3.20; N, 10.68%.

Di- μ -chloro-dichloro[1,3,5-bis(3,5-di-*tert*-butylpyrazolyl)-1-carbonyl]benzene]dipalladium(II) (4)

To a solution of [PdCl₂(NCMe)₂] (0.25 g, 0.96 mmol) in CH₂Cl₂ (40 mL), was added 0.34 g (0.48 mmol) of **L5**. A red, homogeneous solution formed immediately. After stirring overnight, the solvent was evaporated to give a red residue, which was recrystallized from CH₂Cl₂-hexane to give a red powder. Yield = 0.48 g, 94%. Anal. Calc. for C₄₂H₆₀Cl₄N₆O₃Pd₂: C, 47.97; H, 5.75; N, 7.99. Found: C, 47.56; H, 6.10; N, 7.09%. ¹H NMR (CDCl₃): δ 9.50 (d, 2H, Ph, ³J_{HH} = 1.8 Hz); 8.49 (t, 1H, Ph, ³J_{HH} = 1.6 Hz); 6.35 (s, 2H, 4-pyrazole); 6.22 (s, 1H, 4-pyrazole); 1.81 (s, 18H, 5-^tBu); 1.57 (s, 9H, 5-^tBu); 1.48 (s, 18H, 3-^tBu); 1.24 (s, 9H, 3-^tBu). ¹³C{¹H} NMR (CDCl₃): δ 168.6, 168.3, 164.8, 163.8, 158.8, 142.4, 138.5, 138.4, 133.3, 109.8, 106.7, 33.7, 33.4, 31.4, 30.4, 29.9.

General procedure for polymerisation of ethylene

Polymerisation was carried out in a 300 mL stainless steel autoclave, which was loaded with the catalyst and co-catalyst, methylaluminoxane (MAO), in a nitrogen purged glove box. This was done as follows: the autoclave was charged with a palladium complex in dry toluene (150 mL), and appropriate amount of MAO (10% in toluene) (Al: Pd = 1000:1) was added in a glove box. The reactor was sealed and removed from the glove box. The autoclave was flushed three times with ethylene and heated to the polymerization temperature. Ethylene was continuously supplied to maintain constant pressure during the polymerization. After the set experiment time, excess ethylene was vented and the polymerization quenched by adding ethanol. The polymer was filtered off, washed with 2 M HCl followed by ethanol. It was dried in an oven overnight at 50 °C under vacuum.

X-Ray structural determination

Crystal evaluation and data collection were performed on a Bruker CCD-1000 diffractometer with Mo-K α (λ = 0.71073 Å) radiation and the diffractometer to crystal distance of 4.9 cm. Crystal data, data collection, and refinement parameters are listed in Tables 1 and 2. The initial cell constants were obtained from three series of ω -scans at different starting angles. The reflections were successfully indexed by an automated indexing routine built in the SMART program. These highly redundant datasets were corrected for Lorentz and polarization effects. The absorption correction was based on fitting a function to the empirical transmission surface as sampled by multiple equivalent measurements.¹⁷ The structures were solved by direct methods and refined by least-squares techniques using the SHELXTL program.¹⁸ All non-hydrogen atoms were refined with anisotropic displacement coefficients. All hydrogen atoms were included in the structure factor calculation at idealized positions and were allowed to ride on the neighbouring atoms with relative isotropic displacement coefficients.

CCDC reference numbers 178094, 178095, 178097 and 185333–185338.

See <http://www.rsc.org/suppdata/dt/b2/b208376k/> for crystallographic data in CIF or other electronic format.

Results and discussion

Synthesis of ligands

Compounds **L1–L6** were synthesized according to Scheme 1 from the reaction of 1,3-benzenedicarbonyl dichloride (**L1–L3**), 1,2-benzenedicarbonyl dichloride (**L4**), or 1,3,5-benzenetricarbonyl trichloride (**L5** and **L6**) and two (three in case of **L5** and **L6**) equivalents of the appropriate pyrazole.

Table 1 Crystal data and structure refinement for **L1**, **L2**, **L3**, **L4**, **L5** and **L6**

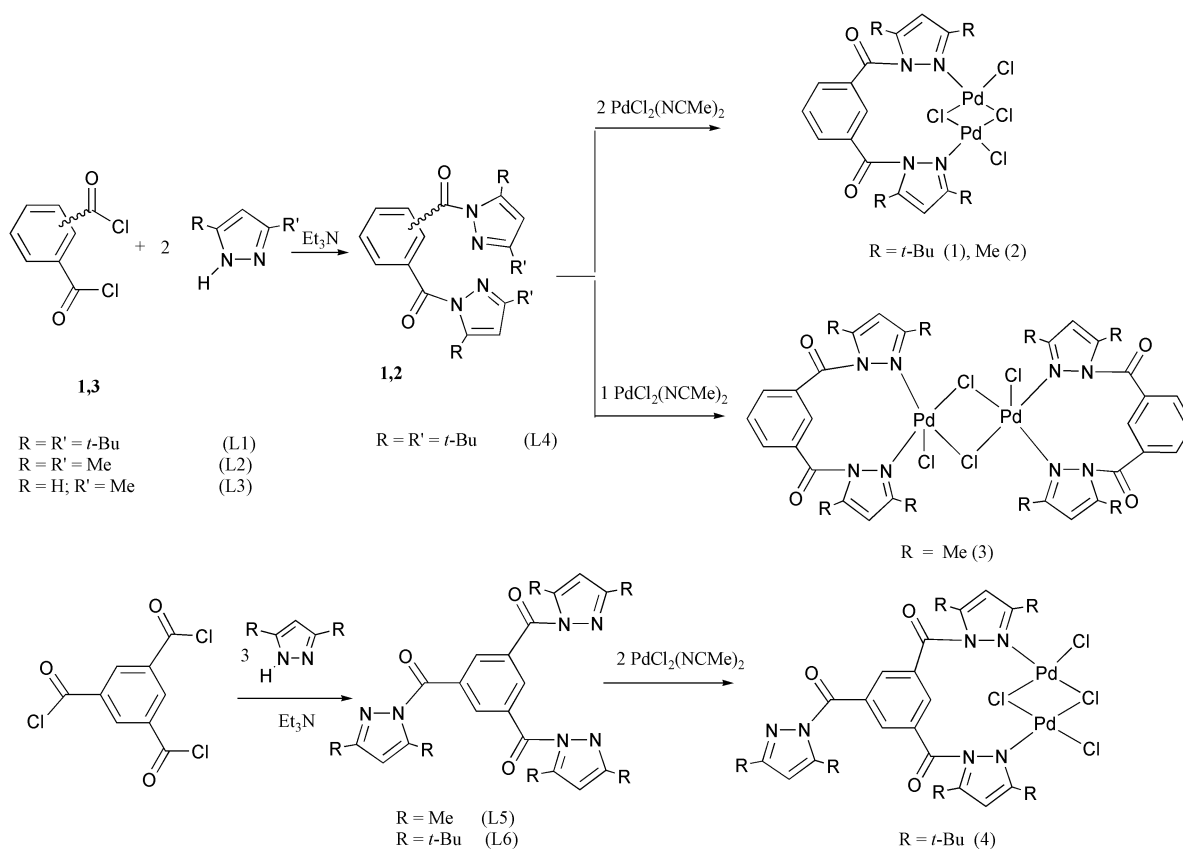
	L1	L2	L3	L4	L5	L6
Empirical formula	C ₃₀ H ₄₂ N ₄ O ₂	C ₁₈ H ₁₈ N ₄ O ₂	C ₁₆ H ₁₄ N ₄ O ₂	C ₃₀ H ₄₂ N ₄ O ₂	C ₄₂ H ₆₀ N ₆ O ₃	C ₃₄ H ₃₄ N ₆ O ₃ ·0.5CHCl ₃
Formula weight	490.68	322.36	294.31	490.68	696.96	504.68
Temperature/K	173 (2)	296 (2)	296 (2)	173 (2)	173 (2)	296 (2)
Crystal system	Monoclinic	Triclinic	Monoclinic	Monoclinic	Orthorhombic	Monoclinic
Space group	<i>P2₁/c</i>	<i>P1</i>	<i>C2/c</i>	<i>P2₁/n</i>	<i>Pbca</i>	<i>C2/c</i>
<i>a</i> /Å	11.0518(8)	8.6173(9)	18.538(2)	11.2718(11)	19.3167(13)	23.360(2)
<i>b</i> /Å	25.9439(19)	9.7287(9)	7.2850(7)	18.6937(18)	14.3940(11)	17.3164(15)
<i>c</i> /Å	10.0002(7)	11.6949(12)	11.3601(13)	13.9240(15)	29.844(2)	16.6335(15)
<i>a</i> ^o	90.0	68.665(3)	90.0	90.0	90.0	90.0
<i>b</i> ^o	92.363(1)	73.638(2)	100.922(2)	95.554(2)	90.0	128.107(1)
<i>c</i> ^o	90.0	63.788(2)	90.0	90.0	90.0	90.0
<i>V</i> /Å ³	2864.9(4)	810.70(14)	1506.4(3)	2920.2(5)	8297.8(11)	5294.3(8)
<i>Z</i>	4	2	4	4	8	8
<i>D_c</i> /Mg m ⁻³	1.138	1.321	1.298	1.116	1.116	1.266
μ (Mo-K α)/mm ⁻¹	0.072	0.089	0.089	0.070	0.071	0.231
Crystal size/mm	0.40 × 0.30 × 0.30	0.50 × 0.37 × 0.32	0.45 × 0.43 × 0.41	0.44 × 0.42 × 0.20	0.50 × 0.20 × 0.20	0.38 × 0.32 × 0.29
Diffractometer	CCD-1000	CCD-1000	CCD-1000	CCD-1000	CCD-1000	CCD-1000
Absorption correction	Empirical SADABS	Empirical SADABS	Empirical SADABS	Empirical SADABS	Empirical SADABS	Empirical SADABS
<i>T</i> _{max} / <i>T</i> _{min}	0.9788/0.9718	0.9720/0.9568	0.9643/0.9609	0.9860/0.9696	0.9660/0.9654	0.9360/0.9173
<i>R</i> (<i>F</i>) ^a (%) [<i>I</i> > 2 σ (<i>I</i>)]	4.47	4.17	3.86	4.64	6.57	5.50
<i>R</i> (<i>wF</i>) ^a (%) (all data)	12.41	11.35	10.77	11.86	19.30	12.46

^a Quantity minimized = $R(wF^2) = \Sigma[w(F_o^2 - F_c^2)]/\Sigma[F_o^2]$; $R = \Sigma|F_o - F_c|/\Sigma F_o$; $\Delta = |(F_o - F_c)|$.

Table 2 Crystal data and structure refinement for complexes **1**, **2** and **4**

	1	2	4
Empirical formula	C ₃₀ H ₄₂ Cl ₄ N ₄ O ₂ Pd ₂	C ₁₉ H ₂₀ Cl ₄ N ₄ O ₂ Pd ₂	C ₄₂ H ₆₀ Cl ₄ N ₆ O ₃ Pd ₂ ·4/3CH ₂ Cl ₂
Formula weight	845.28	761.89	1136.49
Temperature/K	173(2)	296(2)	173(2)
Crystal system	Triclinic	Triclinic	Triclinic
Space group	<i>P</i> $\bar{1}$	<i>P</i> $\bar{1}$	<i>P</i> $\bar{1}$
<i>a</i> /Å	11.8754(10)	11.4285(11)	10.6994(6)
<i>b</i> /Å	12.1953(10)	11.5080(11)	14.6275(7)
<i>c</i> /Å	14.4906(13)	11.9381(12)	17.7885(10)
<i>a</i> °	86.828(2)	100.520(2)	72.212(1)
<i>β</i> °	72.340(2)	118.329(2)	86.365(1)
<i>γ</i> °	63.363(2)	98.458(2)	81.477(1)
<i>V</i> /Å ³	1779.4(3)	1308.3(2)	2621.1(2)
<i>Z</i>	2	2	2
<i>D</i> _c /Mg m ⁻³	1.578	1.934	1.440
<i>μ</i> (Mo-Kα)/mm ⁻¹	1.343	2.012	1.033
Crystal size/mm	0.40 × 0.30 × 0.20	0.25 × 0.20 × 0.06	0.40 × 0.40 × 0.20
Diffractometer	CCD-1000	P4/CCD 1K	P4/CCD 1K
Absorption correction	Empirical	Empirical	Empirical
<i>T</i> _{max} / <i>T</i> _{min}	0.7750/0.6157	0.8888/0.6332	0.8201/0.6828
<i>R</i> (<i>F</i>) ^a (%) [<i>I</i> > 2σ(<i>I</i>)]	3.41	4.07	4.83
<i>R</i> (<i>wF</i> ²) ^a (%) (all data)	11.04	10.90	13.06

^a Quantity minimized = $R(wF^2) = \sum[w(F_o^2 - F_c^2)] / \sum[(wF_o^2)^2]^{1/2}$; $R = \sum \Delta / \sum (F_o)$, $\Delta = |F_o - F_c|$.



Examination of the ¹H NMR spectra of compounds **L1–L3** reveals the effect of the carbonyl groups on the benzene protons. The signals of the protons on carbon 2 of the benzene linkers show the largest downfield shifts, while the protons of carbon 5 are least affected. Compound **L4** has a typical AA'BB' spin system for the 1,2-benzene linker. These data confirm C₂ symmetry of compounds **L1–L4** in solution.

Solid-state structures of **L1–L6** were determined by single crystal X-ray crystallography. Crystallographic parameters for **L1–L6** are presented in Table 1. The molecular structural diagrams of **L1**, **L4** and **L5** are shown in Figs. 1–3, respectively, while the structural diagrams of **L2**, **L3** and **L6** are deposited as

ESI.† All bond distances and angles in the six structures fall within the expected ranges while some torsion angles deserve special discussion, *vide infra*. The structures of the 1,3-(3,5-R₂pzC(O))₂C₆H₄ and 1,2-(3,5-R₂pzC(O))₂C₆H₄ compounds in the solid state can possess either C₂ or C_s symmetry. Hypothetically, a C_{2v} arrangement is conceivable for a highly strained molecule but since this is not realistic and it will not be considered here. In solution, the pyrazolyl-1-ylcarbonyl benzene rings substituents are enantiotopic. The C₂ symmetry is attained when the pz substituents on the benzene ring reside on the opposite sides of its plane. The C_s symmetry is observed when both substituents are on the same side of the ring with the

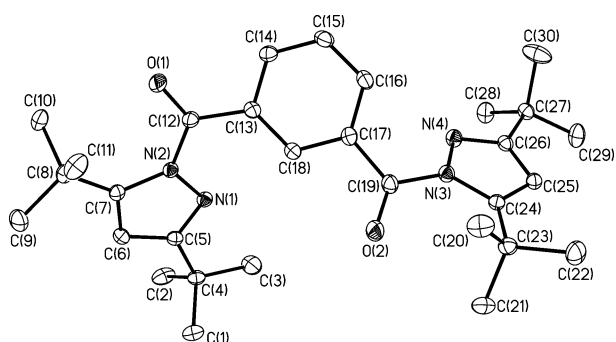


Fig. 1 Molecular drawing of **L1** shown with 30% probability ellipsoids. The hydrogen atoms are omitted for clarity. Selected bond lengths [Å] and angles [°]: N(1)–N(2), 1.3889(14); N(3)–N(4), 1.3837(15); N(2)–C(12), 1.4057(16); N(3)–C(19), 1.4186(17); O(1)–C(12), 1.2098(16); O(2)–C(19), 1.2060(17); C(12)–C(13), 1.4952(18); C(17)–C(19), 1.4966(19); N(1)–N(2)–C(12), 118.16(10); N(4)–N(3)–C(19), 116.67(10); O(1)–C(12)–N(2), 120.30(12); N(2)–C(12)–C(13), 119.80(11); O(1)–C(12)–C(13), 119.90(12); O(2)–C(19)–C(17), 121.95(12); O(2)–C(19)–N(3), 120.39(12); N(3)–C(19)–C(17), 117.66(11).

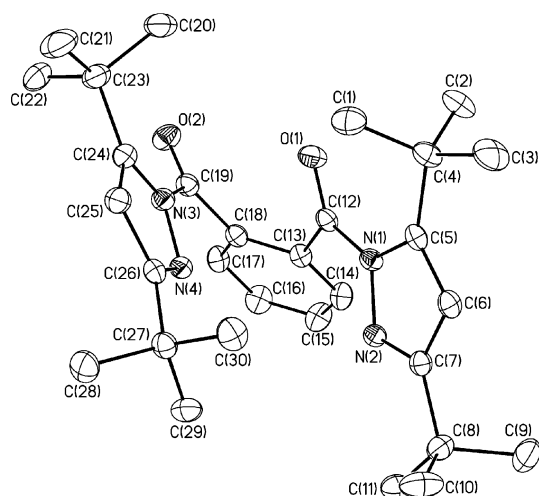


Fig. 2 Molecular drawing of **L4** shown with 30% probability ellipsoids. The hydrogen atoms are omitted for clarity. Selected bond lengths [Å] and angles [°]: N(1)–N(2), 1.3894(18); N(3)–N(4), 1.3779(19); N(1)–C(5), 1.407(2); N(3)–C(24), 1.393(2); O(1)–C(12), 1.212(2); O(2)–C(19), 1.205(2); C(18)–C(19), 1.503(2); C(12)–C(13), 1.490(2); N(2)–N(1)–C(7), 117.59(13); N(4)–N(3)–C(19), 116.18(13); O(1)–C(12)–C(13), 120.07(15); O(2)–C(19)–C(18), 120.82(16); O(1)–C(12)–N(1), 121.06(15); O(2)–C(19)–N(3), 122.71(16); N(1)–C(12)–C(13), 118.86(14); N(3)–C(19)–C(18), 116.36(14).

mirror plane perpendicular to the plane of the ring. Molecular modeling calculations with the MMFFs force field performed on the simplified model of these compounds, 1,3-(3,5-H₂pzC(O))₂C₆H₄, indicated that these two symmetrical conformations are energetically equivalent and are close in energy to a number of calculated energetic minima corresponding to various C_i arrangements. Thus, the spatial arrangement observed in the solid state depends strongly upon the intermolecular interactions in the lattice as well as on packing forces. The X-ray single crystal structural analysis concurs with this assessment.

The structure of **L3** possesses crystallographic two-fold symmetry (molecular symmetry C₂) while the structures of **L1**, **L2** and **L4** are not symmetrical in the solid state (molecular symmetry C_i). Interestingly, the pz substituents in **L1**, **L2** and **L4** are on the same side of the benzene ring in an arrangement that is closer to the C_s symmetry than to C₂. One additional structural feature of **L3** to be noted is the asymmetrical substitution of the pz ligands with the Me group being in the 3 position. In solution, 3-MepzH and 5-MepzH are indistinguishable due to a dynamic equilibrium between these

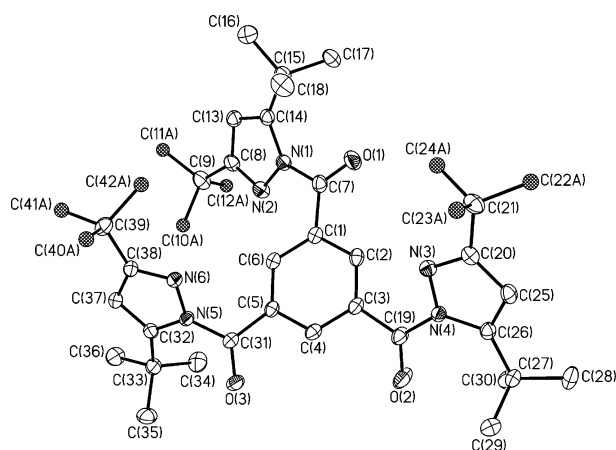


Fig. 3 Molecular drawing of **L5** with the preferred orientations of the disordered groups shown with 30% probability ellipsoids. The hydrogen atoms are omitted for clarity. Selected bond lengths [Å] and angles [°]: N(1)–N(2), 1.387(3); N(3)–N(4), 1.385(3); N(5)–N(6), 1.382(3); N(1)–C(7), 1.423(3); N(4)–C(19), 1.404(3); N(5)–C(31), 1.409(3); O(1)–C(7), 1.205(3); O(2)–C(19), 1.209(3); O(3)–C(31), 1.210(3); C(1)–C(7), 1.494(4); C(3)–C(19), 1.497(4); C(5)–C(31), 1.493(3); N(2)–N(1)–C(7), 117.5(2); N(3)–N(4)–C(19), 116.77(19); N(6)–N(5)–C(31), 116.63(2); O(1)–C(7)–N(1), 120.1(2); O(1)–C(7)–C(1), 121.4(2); N(1)–C(7)–C(1), 118.4(2); O(2)–C(19)–N(4), 120.8(2); O(2)–C(19)–C(3), 120.3(2); N(4)–C(19)–C(3), 118.9(2); O(3)–C(31)–N(5), 120.6(2); O(3)–C(31)–C(5), 121.6(2); N(5)–C(31)–C(5), 117.8(2).

tautomers. Therefore, during the synthesis of **L3** the least sterically hindered product was formed.

The structures of **L5** and **L6** can exist in a variety of energetically similar conformations as revealed by the results of molecular modeling calculations carried out on a simplified analogue molecule 1,3,5-(3,5-H₂pzC(O))₃C₆H₃. Its highest symmetry attainable without inducing considerable steric repulsion between the bulky substituent is C₃ with the three pz substituents tilted in the same fashion relative to the benzene ring. It is also possible to envision a C_s arrangement when the mirror plane contains one pz substituent and dissects the phenyl ring through the carbons bearing this substituent and the carbon in the *para* position while the other substituents arranged as mirror images across this mirror. Neither however is observed in the solid-state structures of **L5** and **L6** as both molecules are asymmetrical. It is worth mentioning that in compound **L5** all three pz substituents are on the same side of the benzene ring (pseudo-C₃ symmetry) while in **L6** two substituents are on one side of the ring and the third one is on the other.

There are several common features shared by **L1**–**L6**. In all these molecules the configuration about the single bond C–N in the O=C–N–N linkage is inevitably *E*. This spatial arrangement maximizes delocalization of the electron density between the carbonyl and the pz ring. It is important to notice that while benzaldehyde is planar, compounds **L1**–**L6** cannot achieve planarity due to either close proximity of the pyrazolyl substituent in the 2-position to the *ortho* hydrogen of the phenyl ring, or due to unfavorable interactions between the nitrogen lone pair and the *ortho* hydrogen. Thus, a conjugated system delocalized over the two rings and the carbonyl cannot be attained. The C=O group can, however, be coplanar with either ring since both pyrazolyl and phenyl groups possess a delocalized π-system. The preferred ring is the pyrazole.

The C–N bond in the O=C–N–N linkage is expected to be shorter than the generic C_{sp²}–N_{sp²} single bond due to electronic resonance. The C–N bond is the shortest when the torsion angle O–C–N–N is 180° and longest when the angle is 90°. The length of the C–N bond can ideally be described as a cosine function of the O=C–N–N torsion angle. Fig. 4 shows the dependence of the C–N bond distance in the free ligand O=C–N–N linkage on the O=C–N–N torsion angle. It represents 14 values observed in

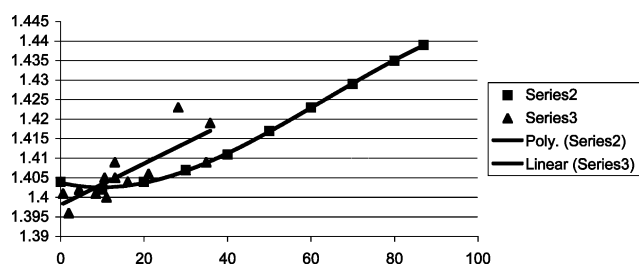


Fig. 4 Dependence of the C–N bond distance in the free ligand O=C–N–N linkage on the O=C–N–N torsion angle. The abscissa shows the value of the O=C–N–N torsion angle while the ordinate is the corresponding C–N bond length. The squares show the theoretical and triangles the experimentally observed values.

L1–L6 and several theoretical values obtained by performing MMFFs calculations on 3,5- $H_2pz-C(O)-Ph$.

An attempt to parameterize the conformations of the molecules by considering torsion angles O=C–C–C and O=C–N–N as well as the dihedral angle between the pz and Ph planes, did not reveal any systematic trend. MMFFs calculations confirmed that the most energetically favorable conformations are those in which the carbonyl is coplanar with the pz ring. The experimentally observed values in Fig. 4 lie above the theoretically calculated values, but the differences are not statistically significant and are accounted for by the standard uncertainties intrinsic to the X-ray single crystal analysis and the actual substitution pattern. The dihedral angles between the pz and Ph planes in **L1–L6** were about 30° regardless of the substituents on the pyrazole.

Synthesis of metal complexes

Compounds **L1** and **L2** react with $[PdCl_2(NCMe)_2]$ in a 1:2 ratio to form red Pd complexes **1** and **2** (Scheme 1) in high yields, whereas a similar reaction with **L3** gave intractable materials. These complexes were characterized by multinuclear NMR spectroscopy, elemental analysis and single crystal X-ray analyses. The reaction between **L2** and $[PdCl_2(NCMe)_2]$ in a 1:1 ratio yielded complex **3**, which, once isolated, became insoluble in common organic solvents such as CH_2Cl_2 , toluene, DMSO and THF. Thus, it was characterized by elemental analysis. Even though complex **3** is formulated as a dimeric structure (Scheme 1) the possibility of it being an oligomer, which could explain its insoluble nature, cannot be discounted. Interestingly, the reaction of **L1** with $[PdCl_2(NCMe)_2]$ in either 1:2 or 1:1 ratios produced exclusively complex **1**. The 1H NMR spectrum of **1** has its most downfield chemical shift associated with protons in positions 4 and 6 of the benzene linker and illustrates that on complexation, **L1** is locked into a rigid framework that does not allow free rotation of the carbonyl functional groups. This is confirmed by the solid state structure of **1** (Fig. 5). The X-ray structures of **1** and **2** show how each pyrazolyl unit in both ligands is bonded to different Pd atoms with the nitrogen atom lone pair. Complexes **1** and **2** are thus stabilized *via* bridging chlorides (Fig. 5).

Complex **4** was synthesized by reacting ligand **L5** with $[PdCl_2(NCMe)_2]$ in a 1:2 ratio (Scheme 1). The 1H NMR of complex **4** showed two types of protons associated with the pyrazolyl groups in a 2:1 intensity ratio. The first type of pyrazolyl group consists of two pyrazolyl units bonded to Pd atoms (6.35 ppm); whereas the second type of pyrazolyl group is not bound (6.22 ppm). The NMR data for **4** and elemental analysis support the proposed formula, which was confirmed by X-ray crystallography (Fig. 6). The reaction of **L6** with $[PdCl_2(NCMe)_2]$, in either a 1:2 or a 1:1 ratio, led to sparingly soluble products which were not further characterised.

In forming the Pd complexes (**1–4**) it is clear from the types of products that the bonding modes of ligands **L1**, **L2** and **L5** are different compared other pyrazolyl ligands.¹⁹ Literature reports show that pyrazolyl units in 1,3,5-tris(pyrazolyl-1-

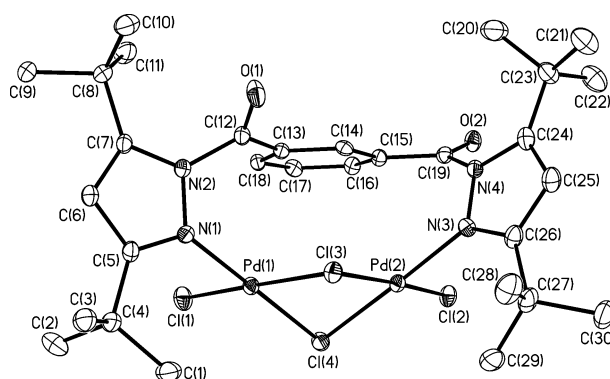


Fig. 5 A molecular drawing of **1** shown with 50% probability ellipsoids. The H atoms are omitted for clarity. Selected bond lengths [Å] and angles [°]: Pd(1)–N(1), 2.029(3); Pd(2)–N(3), 2.040(3); Pd(1)–Cl(1), 2.2683(11); Pd(2)–Cl(2), 2.2647(11); Pd(1)–Cl(4), 2.3094(11); Pd(2)–Cl(4), 2.3031(11); Pd(1)–Cl(3), 2.3640(10); Pd(2)–Cl(3), 2.3844(11); Pd(1)–Pd(2), 3.2117(5); N(1)–Pd(1)–Cl(1), 89.08(10); N(3)–Pd(2)–Cl(4), 178.22(10); N(1)–Pd(1)–Cl(4), 179.17(10); Cl(2)–Pd(2)–Cl(4), 91.36(4); Cl(1)–Pd(1)–Cl(4), 91.49(4); N(3)–Pd(2)–Cl(3), 93.19(10); N(1)–Pd(1)–Cl(3), 93.69(10); Cl(2)–Pd(2)–Cl(3), 176.78(4); Cl(1)–Pd(1)–Cl(3), 176.99(4); Cl(4)–Pd(2)–Cl(3), 85.43(4); Cl(4)–Pd(1)–Cl(3), 85.76(4).

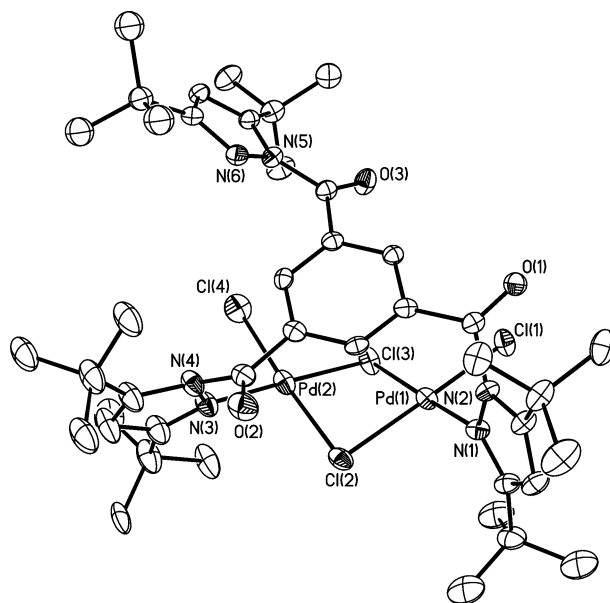


Fig. 6 A molecular drawing of **4** shown with 50% probability ellipsoids. The H atoms are omitted for clarity. Selected bond lengths [Å] and angles [°]: Pd(1)–N(1), 2.030(4); Pd(2)–N(3), 2.033(4); Pd(1)–Cl(1), 2.2564(13); Pd(2)–Cl(2), 2.2789(17); Pd(1)–Cl(4), 2.3669(13); Pd(2)–Cl(4), 2.3418(15); Pd(1)–Cl(3), 2.3023(13); Pd(2)–Cl(3), 2.3074(13); Pd(1)–Pd(2), 3.2569(6); N(1)–Pd(1)–Cl(1), 89.89(12); N(3)–Pd(2)–Cl(3), 178.36(15); N(1)–Pd(1)–Cl(3), 174.96(10); Cl(2)–Pd(2)–Cl(3), 91.22(6); Cl(1)–Pd(1)–Cl(3), 91.17(5); N(3)–Pd(2)–Cl(4), 93.08(15); N(1)–Pd(1)–Cl(4), 94.69(10); Cl(2)–Pd(2)–Cl(4), 175.30(4); Cl(1)–Pd(1)–Cl(4), 175.30(5); Cl(3)–Pd(2)–Cl(4), 85.28(4); Cl(4)–Pd(1)–Cl(3), 84.82(5).

ylmethyl)benzene^{19a} and 1,3,5-tris(pyrazolyl-1-ylmethyl)benzene^{19b} form complexes that have only one metal bonded to two pyrazolyl units, contrary to what we observed in complexes **1**, **2** and **4**. The bonding mode in **L1**, **L2** and **L5** to palladium is likely to be determined by two main factors, namely electro-withdrawing groups on the linkers and steric hindrance by the substituents on the pyrazolyl units. In experiments performed with $[PdClMe(cod)]$ as a source of palladium, ligands **L1**, **L2** and **L5** were unable to displace cod in $[PdClMe(cod)]$ to form the corresponding pyrazolyl palladium complex. The above results also indicate that the pyrazolyl compounds **L1**, **L2** and **L5** are weaker donors than 3,5-Me₂pz and 3,5-^tBu₂pz which readily react with $[PdCl_2(cod)]$ to form $[Pd(3,5-R_2pz)_2Cl_2]$

Table 3 Ethylene polymerisation data and conditions^a

Expt.	Cat.	Pressure/atm	TON/kg mol ⁻¹ h ⁻¹	Mp/°C (DSC)	M _n (×10 ⁵)	M _w (×10 ⁵)	M _w /M _n
1	1	5	2591.4	136.04	4.420	9.130	2.04
2	1	1	1843.0	136.80	4.504	9.377	2.08
3	2	5	503.0	136.31	4.569	9.384	2.05
4	2	1	392.9	136.58	4.631	9.727	2.10
5	4	5	1099.2	136.53	4.369	9.018	2.06
6	4	1	215.2	136.08	4.514	9.550	2.12

^a [Pd] = 12.5 × 10⁻⁶ M; Al: Pd = 1000:1; polymerization temperature = 30 °C; polymerisation time = 30 min.

(R = Me, ^tBu) and [Pd(3,5-^tBu₂pz)₂Cl(Me)], respectively.²⁰ Further evidence that **L1**, **L2** and **L5** are weakly bonded to Pd in **1–4** complexes is provided by the reaction of these complexes with known weak ligands like thiophene and tetrahydrothiophene. We were able to isolate free pyrazolyl ligands in such reactions. For example the reaction of complex **1** with pyridine produced [Pd₂(py)₂Cl₄] within 5 min, a product characterised by ¹H NMR and elemental analysis,²¹ which demonstrates how weakly bonded **L1** is in complex **1**. We believe the relatively weak donor ability of the ligands **L1**, **L2** and **L5**, compared to other pyrazolyl or pyridine derivatives as ligands, makes the Pd centres in the complexes formed by **L1**, **L2** and **L5** more electrophilic; a hypothesis we are using to investigate the ability of cations of **1** to form phenylacetylene complexes.

Whereas compounds **L1**, **L2** and **L5** formed soluble products, **L3** and **L6** formed insoluble or sparingly soluble products, respectively, whilst **L4** did not react at all. It is likely that the inability of **L4** to form a complex is due the steric bulk of the *tert*-butyl substituents on the pyrazolyl units, thus leaving no room for the two PdCl₂ units required to form a complex.

The molecular structures of **1** and **4** are presented in Figs. 5 and 6, and crystallographic information for **1**, **2** and **4** is tabulated in Table 2. The Pd atoms in the dinuclear complexes **1**, **2** and **4** are in slightly distorted square planar configurations with the bond angles about the Pd atoms ranging between 84.35(5) and 94.68(12)°. Each Pd metal and the four atoms comprising its coordination sphere, three chlorines and one nitrogen, are planar within 0.07 Å in the three complexes. The Pd–Cl(terminal), Pd–Cl(bridging *trans* to N) and Pd–Cl(bridging *trans* to Cl), bond lengths in **1**, **2** and **4** average to 2.266(8), 2.305(4) and 2.360(15) Å, respectively, and fall within the usual ranges for these interactions. The disparity between the metal–chlorine distances to the bridging atoms warrants special mentioning. The *trans* influence of the pyrazolato ligands as a good π-donor is not reflected in these structures. The metal–chloride distance *trans* to the pz ligand is shorter as the latter is a weaker σ-donor than the chloride. The average Pd–N bond distance in **1**, **2** and **4** (2.032(5) Å) is somewhat shorter than the average value of 2.1(1) Å calculated for 59 Pd–N(pz) bond lengths reported to the Cambridge Structural Database (CSD),²² however the difference is not statistically significant.

The unique feature of **1**, **2** and **4** that sets them apart from all but one other dinuclear Pd complexes with the L₂Pd(μ₂-Cl)₂-PdL₂ core is the smaller dihedral angle between the planes defined by the Pd centres and two bridging Cl atoms. Thus, the angle between planes Pd(1)–Cl(3)–Cl(4) and Pd(2)–Cl(3)–Cl(4) spans 136.31(5), 138.61(5) and 143.11(7)° in **1**, **2** and **4**, respectively. This folding shortens the Pd–Pd separation to 3.2004(6), 3.2117(5) and 3.2569(6) Å, correspondingly. Undoubtedly, such strained ligand arrangement stems from the incorporation of a bidentate bridging ligand into the system. The only other Pd complex with similar geometry [Pd₂Cl₄((*R,R*)-1,5-bis-*o*-(*p*-toluenesulfinyl)phenoxy)-3-oxapentane)](CH₂Cl₂)₂ was reported by Hambley *et al.* in 1985.^{5d} There the corresponding parameters measured 139.0° and 3.280(1) Å. In 21 other relevant complexes reported to the CSD the Pd–μ₂-Cl₂-Pd rhombuses were planar with the Pd–Pd distances averaging 3.45(5) Å.

The presence of conformational tension in the bridging ligands also manifests itself in the values of the O=C–N–N torsion angles. The carbonyl groups link two aromatic systems, the pyrazole ring and benzene moiety. It has been demonstrated, from the ligand structures discussed earlier, that the free ligands **L1** and **L2** cannot be planar due to steric considerations, but the carbonyl group is usually coplanar with the pyrazolato ring with the *E* configuration about the O=C–N–N bond. The expected torsion angle O=C–N–N is 180°. However, all experimentally observed values are considerably different in **1** (O(2)–C(6)–N(2)–N(1) 147.0(5)°; O(1)–C(13)–N(4)–N(3) 134.1(5)°), **2** (O(1)–C(12)–N(2)–N(1) 115.1(4)°; O(2)–C(19)–N(4)–N(3) 122.5(4)°) and **4** (O(1)–C(12)–N(2)–N(1) 119.1(5)°; O(2)–C(19)–N(4)–N(3) 119.6(6)°). The torsion angle closest to linearity is found for the one uncoordinated pyrazole in **4** (O(3)–C(31)–N(5)–N(6) (158.3(5)°)). The carbonyl vectors are not coplanar with the benzene rings either, which is in accord with the conformation of the free ligands in the solid state. Consequently, the coordination of the pyrazolato nitrogen atoms to palladium metal centres is strong enough to cause significant puckering of the ligand and yet accommodate it as a bridging moiety. In addition, molecules **1**, **2** and **4** deviate significantly from the possible C_s symmetry.

Ethylene polymerisation

Ethylene polymerisation reactions were performed with complexes **1**, **2** and **4** using MAO as co-catalyst. The results of the polymerisation are in Table 3. Polymerization was performed at 5 atm and 1 atm, with catalytic activity at 5 atm substantially higher. The catalytic activity was found to decrease in the order **1** > **4** > **2**. Whilst **1** and **4** have good solubility in toluene, **2** has a low solubility in toluene. This low solubility of **2** is likely to be the cause of its low activity.

The polymers were characterised by a combination of high temperature ¹³C NMR, high temperature gel permeation chromatograph (GPC) and by thermal analysis (TGA DSC). Polyethylene isolated in these experiments had melting points of about 136 °C and a single ¹³C NMR peak characteristic of high density polyethylene (HDPE). The catalytic activity of **1** was about twice that of **4**. It was also about the same magnitude more active than [Pd(3,5-^tBu₂pz)₂Cl₂]²⁰ (TON = 1005.7 kg mol⁻¹ h⁻¹). Quite clearly the presence of carbonyl groups in the pyrazolyl ligands in **1** improves its electrophilic behaviour and hence its catalytic activity compared to [Pd(3,5-^tBu₂pz)₂Cl₂]. We expected **4** to have a similar catalytic activity to **1** since the coordination environment of the active metal species for polymerization in both **1** and **4** are the same. The lower activity of **4** could be due to the presence of the non-coordinating pyrazolyl unit, which could be complexing with the co-catalyst MAO, thus reducing the amount of active palladium catalyst available for the polymerization. Formation of an Al–pyrazolyl adduct when MAO is used to activate **4** is feasible as Al–NR₃ adducts are well known.²³ Examples of pyrazolyl–Al compounds have also been reported in the literature [Al(1,3,5-Me₃pz)₂]²⁴ and [Tp*₂Al][AlCl₄].^{4d} Though all three catalysts have a reasonable catalytic activity, they appear to deactivate over time. The deactivation is probably the result of ligand dis-

sociation from the metal centre. The possibility of the active catalyst being a ligand–Al compound, formed from a dissociated ligand and MAO, can be discounted; since a blank polymerisation reaction performed with **L1** and MAO (1:1000) at ethylene pressure of 5 atm and 30 °C gave only a small amount of polymer.

The results of the polymerization studies demonstrate that fine-tuning the electrophilicity of the palladium centre in pyrazolyl complexes catalysts should lead to highly active olefin polymerization catalysts. However a balance between the stability of the catalyst and its electrophilic behaviour has to be found. We are currently investigating this.

Conclusions

A series of six compounds with pz rings connected with benzenedicarbonyl and benzenetricarbonyl have been prepared and fully analytically characterized. The presence of the carbonyl functional groups reduce the σ -donor ability of the nitrogen atoms of the pz ligands. When activated with MAO, Pd complexes with these ligands show activity in ethylene polymerization. The reduced σ -donor ability of ligands **L1–L6** may play a role in the catalytic process as it facilitates the break of the Pd–N bonds to assist coordination of the substrate to the metal center. Further studies of the polymerization process will be presented in a future report.

Acknowledgements

This work was supported by the National Research Foundation (South Africa). We thank SASOL polymers for the high temperature GPC data.

References and notes

- 1 T. N. Sorrell, in *Biological and Inorganic Copper Chemistry*, ed. K. D. Karlin and J. Zubieta, Academic Press, New York, 1986, vol. 2, p. 41.
- 2 (a) W. H. Armstrong, A. Spool, G. C. Papaefthymion, R. B. Franked and S. J. Lippard, *J. Am. Chem. Soc.*, 1984, **106**, 3653; (b) J. S. Thompson, T. J. Marks and J. A. Ibers, *J. Am. Chem. Soc.*, 1979, **101**, 4180; (c) C. Kimblin, B. M. Bridgewater, D. G. Churchill, T. Hascall and G. Parkin, *Inorg. Chem.*, 2000, **39**, 4240; (d) S.-J. Chion, J. Innocent, C. G. Riordan, K.-C. Lam, L. Liable-Sands and A. L. Rheingold, *Inorg. Chem.*, 2000, **39**, 4347; (e) C. C. Tang, D. Davalian, P. Huang and R. Breslow, *J. Am. Chem. Soc.*, 1978, **100**, 3918; (f) R. S. Brown and J. Huguet, *Can. J. Chem.*, 1980, **58**, 889.
- 3 S. Komeda, M. Lutz, A. L. Spek, M. Chikuma and J. Reedijk, *Inorg. Chem.*, 2000, **39**, 4230.
- 4 (a) S. Trofimenko, *Chem. Rev.*, 1972, **72**, 497; (b) S. Trofimenko, *Prog. Inorg. Chem.*, 1986, **34**, 115; (c) K. Niedenzu and S. Trofimenko, *Top. Curr. Chem.*, 1986, **131**, 1; (d) S. Trofimenko, *Chem. Rev.*, 1993, **93**, 943; (e) F. Mani, *Coord. Chem. Rev.*, 1992, **120**, 325.
- 5 (a) T. A. Hafeli and F. R. Keene, *Aust. J. Chem.*, 1988, **41**, 1379; (b) P. K. Byers, J. Canty, B. W. Skelton and A. H. White, *J. Chem. Soc., Chem. Commun.*, 1987, **1**, 93; (c) P. K. Byers, J. Canty, B. W. Skelton and A. H. White, *Organometallics*, 1990, **9**, 826; (d) T. W. Hambley, B. Raguse and D. D. Ridley, *Aust. J. Chem.*, 1985, **38**, 1445.
- 6 F. Mani and G. Scapacci, *Inorg. Chim. Acta*, 1980, **38**, 151.
- 7 (a) W. L. Driessen, *Rect. Trav. Chim. Pays-Bas*, 1982, **101**, 441; (b) J. B. J. Veldhuis, W. L. Driessen and J. Reedijk, *J. Chem. Soc., Dalton Trans.*, 1986, 537; (c) J. W. F. M. Schoonhoven, W. L. Driessen, J. Reedijk and G.-C. Verschoor, *J. Chem. Soc., Dalton Trans.*, 1984, 1053; (d) H. L. Blonk, W. L. Driessen and J. Reedijk, *J. Chem. Soc., Dalton Trans.*, 1985, 1699; (e) G. J. Van Driel, W. L. Driessen and J. Reedijk, *Inorg. Chem.*, 1985, **24**, 2914; (f) W. G. Haanstra, W. L. Driessen, J. Reedijk, U. Turperinen and R. Hamalainen, *J. Chem. Soc., Dalton Trans.*, 1989, 2309.
- 8 (a) T. N. Sorrell, C. J. O'Connor, O. P. Anderson and J. H. Reibenspies, *J. Am. Chem. Soc.*, 1985, **107**, 4199; (b) T. N. Sorrell, M. R. Malachowski and D. L. Jameson, *Inorg. Chem.*, 1982, **21**, 3250; (c) T. N. Sorrell and V. A. Vankai, *Inorg. Chem.*, 1990, **29**, 1687; (d) T. N. Sorrell, V. A. Vankai and M. L. Garrity, *Inorg. Chem.*, 1991, **30**, 207.
- 9 G. Dong, J. P. Matthews, D. C. Craig and A. T. Baker, *Inorg. Chim. Acta*, 1999, **284**, 266.
- 10 C. M. Hartshorn and P. J. Steel, *Organometallics*, 1998, **17**, 3487.
- 11 C. M. Hartshorn and P. J. Steel, *Aust. J. Chem.*, 1995, **48**, 1585.
- 12 (a) K. R. J. Thomas, V. Chandrasekhar, C. D. Bryan and A. W. Cordes, *J. Coord. Chem.*, 1995, **35**, 337; (b) K. R. J. Thomas, P. Tharmaraj, V. Chandrasekhar and E. R. T. Tiekink, *J. Chem. Soc., Dalton Trans.*, 1994, 1301; (c) K. R. J. Thomas, V. Chandrasekhar, P. Pal. S. R. Scott, R. Hallford and A. W. Cordes, *Inorg. Chem.*, 1993, **32**, 606; (d) K. R. J. Thomas, *Acta Crystallogr., Sect. C*, 1998, **54**, 331.
- 13 (a) A. Chandrasekaran, S. S. Khrisnamurthy and M. Nethaji, *J. Chem. Soc., Dalton Trans.*, 1994, 63; (b) K. D. Gallicano and N. L. Paddock, *Can. J. Chem.*, 1982, **60**, 521.
- 14 (a) L. L. Blosch, K. Abbound and J. M. Boncella, *J. Am. Chem. Soc.*, 1991, **113**, 7067; (b) S. Tsuji, D. C. Swenson and R. F. Jordan, *Organometallics*, 1999, **18**, 4758.
- 15 (a) C. K. Gosh, D. P. S. Rodgers and W. A. G. Graham, *J. Chem. Soc., Chem. Commun.*, 1988, 1511.
- 16 J. Elguero and E. G. R. Jacquier, *Bull. Soc. Chim. Fr.*, 1968, **2**, 707.
- 17 R. H. Blessing, *Acta Crystallogr., Sect. A*, 1995, **51**, 33.
- 18 G. Sheldrick, Bruker SHELXTL (Version 5.1), Analytical X-ray Systems, Madison, WI, 1997.
- 19 (a) C. M. Hartshorn and P. J. Steel, *Chem. Commun.*, 1997, 541; (b) W.-K. Chang, S.-C. Sheu, G.-H. Lee, Y. Wang, T.-I. Ho and Y.-C. Lin, *J. Chem. Soc., Dalton Trans.*, 1993, 687.
- 20 K. Li, I. A. Guzei, J. Darkwa and S. F. Mapolie, *J. Organomet. Chem.*, 2002, **660**, 109.
- 21 (py)₂Pd₂Cl₄: Anal. Calc. for C₁₀H₁₀Cl₄N₂Pd₂: C, 23.42; H, 1.97; N, 5.46. Found: C, 22.06; H, 1.41; N, 5.43%. ¹H NMR (CDCl₃): δ 8.58 (dd, 2H, py, ²J_{HH} = 6.6 Hz, ³J_{HH} = 1.4 Hz); 7.84 (tt, 1H, py, ²J_{HH} = 7.6 Hz, ³J_{HH} = 1.5 Hz); 7.37 (td, 2H, py, ²J_{HH} = 7.6 Hz, ³J_{HH} = 1.6 Hz).
- 22 F. H. Allen and O. Kennard, *Chem. Des. Autom. News*, 1993, **8**, 31.
- 23 (a) J. J. Eisch, in *Comprehensive Organometallic Chemistry II*, ed. E. W. Abel, F. G. A. Stone and G. Wilkinson, Pergamon, 1995, p. 431; (b) F. A. Cotton, G. Wilkinson, C. A. Murillo and M. Bochmann, *Advanced Inorganic Chemistry*, John Wiley & Sons, New York, 6th edn., 1999, p. 196; (c) G. H. Robinson, in *Coordination Chemistry of Aluminum*, ed. G. H. Robinson, VCH, New York, 1993, p. 57.
- 24 I. P. Romm, T. A. Zayakina, V. N. Sheinker, E. N. Guryanova, A. D. Garnovskii and O. Osipov, *Zh. Obshch. Khim.*, 1976, **46**, 2279.